

Quality at the Tail

Zhengxin Yang, Wanling Gao, Chunjie Luo, Lei Wang, Fei Tang, Xu Wen, Jianfeng Zhan*

Research Center for Advanced Computer Systems, Institute of Computing Technology, Chinese Academy of Sciences

University of Chinese Academy of Sciences

{yangzhengxin17z, gaowanling, luochunjie, wanglei_2011, tangfei, wenzu, zhanjianfeng}@ict.ac.cn

Abstract

Benchmarking and evaluating deep learning models and systems necessitate a meticulous approach to ensure comprehensive assessment. In practical applications, it is paramount to consider both the inference quality and the inference time, particularly within safety-critical (e.g., autonomous driving) and mission-critical (e.g., emotion recognition) contexts, where stringent requirements demand the simultaneous satisfaction of both metrics. Neglecting either aspect can result in severe and irreversible consequences, including loss of human life and property damage. Unfortunately, many studies lack a comprehensive consideration of these metrics, often conducted under ideal or permissive conditions, thereby leading to incomplete or non-intuitive evaluation methodologies.

This study reveals a counterintuitive phenomenon: deep learning inference quality exhibits fluctuations due to the influence of inference time, which further introduces complications and challenges to the benchmarking and evaluation. To better depict and characterize the phenomenon, the concept of “tail quality” is introduced, which indicates the quality at the tail of distributions. This paper highlights that “tail quality” can offer a more objective and comprehensive evaluation, overcoming the limitations of conventional inference quality and inference time metrics in capturing the quality fluctuation phenomenon. To capture the phenomenon, this paper also proposes a pioneering, flexible, and customizable evaluation framework for comprehensive assessment and analysis of various factors affecting inference time and quality, such as software and hardware systems, models, and data. Leveraging this framework enables the anticipation of the potential distribution of inference time and inference quality, thus capturing the phenomenon of “tail quality” before practically deploying and applying deep learning. The effectiveness of the evaluation framework is validated through experiments conducted on deep learning models for three different tasks across four systems. Furthermore, employing this evaluation framework, the experiments conducted a preliminary analysis of several factors influencing inference quality and inference time, including the hardware system, deep learning framework, and data.

1. Introduction

Deep learning is catalyzing rapid advancements across a wide range of domains, encompassing areas such as natural lan-

guage processing [6, 30, 38] and computer vision [2, 7, 14, 16]. This surge is paving the way for an escalating deployment of deep learning models and systems in cutting-edge real-world applications such as autonomous driving [3, 19, 34] and smart healthcare [22, 24]. In the face of this expansion across diverse fields, the execution of benchmarking and evaluation is essential to ensure the proper and effective development of these models and systems. Furthermore, within real-world applications, it is paramount to consider the metrics of inference quality and inference time carefully and comprehensively when establishing benchmarking and evaluation methodologies. These metrics reflect the capabilities of deep learning and significantly influence the user experience.

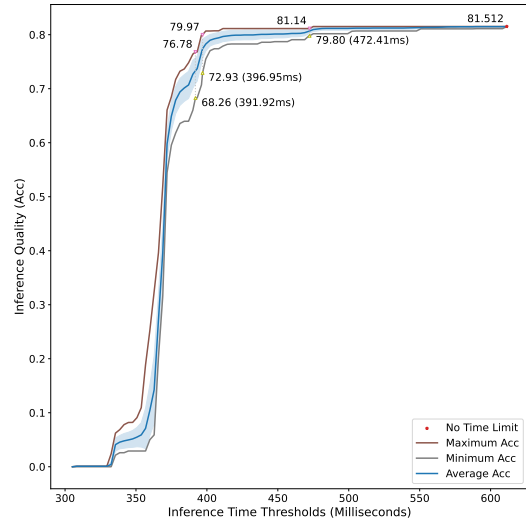


Figure 1: Quality Fluctuations of an Image Classification Model Vision Transformer (ViT). The triangular symbols from left to right represent the maximum and minimum values of inference quality, using the 90th, 95th, and 99th percentiles of tail latency as the inference time thresholds.

Unfortunately, many current studies tend to focus on evaluating only one aspect while neglecting the other and fail to consider the evaluation in real-world applications, especially critical¹ tasks. One significant reason for this issue is that it

¹Based on Sommerville [27], “critical systems” are systems where “system failure may result in injury to people, damage to the environment, or extensive economic losses.” Examples include autonomous driving (safety-critical), business negotiation (business-critical), and navigational system for a spacecraft (mission-critical) [11].

*Corresponding author: Jianfeng Zhan.

is commonly believed that once the neural network model is trained and its parameters are fixed, the inference quality of deep learning on the same data will never change regardless of variations in the deployment environment. However, as this paper is about to reveal, a counterintuitive phenomenon in the practical deployment and application of deep learning is captured, in which fluctuations in inference quality can occur due to variations in inference time, even when the inference inputs remain unchanged. Specifically, for safety-critical tasks like autonomous driving, ensuring high-quality inference while adhering to stringent inference time requirements is of utmost importance. For example, given that humans typically need about 390 to 600 milliseconds to respond to hazards [32, 33], the capability of object detection systems in autonomous driving must surpass human levels[29] within mere tens to hundreds of milliseconds, to reduce the likelihood of accidents. For a specific critical task object detection model, even if the inference time exceeds the specific time constraint by just a few tens of milliseconds, it may have already traveled several meters and caused severe consequences such as loss of life and property damage.

To better illustrate this phenomenon, the authors propose a new term “*tail quality*,” $x\%$ tail quality @ t , which identifies inference quality when we set an $x\%$ tail latency t as the time threshold. For example, we set 99.9% tail latency = ten ms (milliseconds) as the time threshold. If the time of an inference surpasses ten ms, even if its prediction is correct, we still consider it a failure. Its tail quality is written as 99.9% tail quality @10 ms. For a hard real-time system, if the time threshold is 10 ms, its tail quality is written as 100% tail quality @ 10 ms.

In this context, the portion of assessment values where inference quality declines compared to the original inference quality without time constraints is collectively referred to as “tail quality.” Figure 1 provides a more intuitive depiction of the phenomenon. As observed, 99% tail quality @ 472 ms dropped by approximately 1.7 percentage points. However, 90% tail quality @ 392ms plummeted by around 13 percentage points. As the threshold becomes stricter, moving from 400ms to 300ms, the model’s inference quality exhibited significant fluctuations and declined dramatically, eventually reaching an accuracy of 0%. However, such threshold settings are stringent in safety-critical tasks; for instance, tasks like autonomous driving need to achieve high quality when inference times are within a few tens of milliseconds, e.g., 100% tail quality @10 ms is greater than 99.9%. This highlights the severity of the “tail quality” phenomenon. “Tail quality” could have profound implications in real-world scenarios, particularly in contexts like driving, where decisions are constantly made based on rapidly changing traffic conditions. Considering the enormous number of vehicles on the roads daily, if control were to be handed over to a deep learning model, even if the probability of encountering a “tail quality” event (i.e., inference failure) is low, within such a vast population, any decision-making error

arising from such an occurrence could lead to loss of life or property, which is unacceptable.

Many studies have predominantly used individual quality metrics such as *accuracy* [7, 16], *average precision* [2, 8, 20], or individual inference time metrics like *tail latency* [5, 9, 10, 25] to characterize the performance of deep learning. What sets apart the concept of “*tail quality*” is that it allows for a more intuitive depiction of the impact of inference time on inference quality and thus provides insights into the extent of potential consequences caused by inference failures.

Moreover, due to the intricacies of benchmarking in computer science, deep learning software and hardware systems, along with the models that serve as their workloads, are entangled and mutually influential [25, 36]. As a result, conducting a systematic analysis of the causes behind fluctuations in deep learning inference time and inference quality has been challenging. Based on the premise, and with the revelation of “*tail quality*” and its implication of the dependency between inference quality and inference time, benchmarking and evaluation of deep learning inference have become even more complex. However, on the flip side, it also sheds light on establishing comprehensive analyzing methodologies. To this end, the paper proposes a novel evaluation framework that can be flexibly customized according to specific requirements. It systematically analyzes the effects of the entire deployment and application environment of deep learning by disassembling it into several components, such as software and hardware systems, models, and data. Furthermore, statistical methods intuitively depict the approximate distribution of inference time and inference quality under the influence of different components, enabling the prediction of the “tail quality” phenomenon in inference quality before deploying deep learning applications.

Finally, experiments are conducted on frequently used deep learning models for three different tasks across four systems and two deep learning frameworks, where the details of experiments are shown in Table 1 and 2. On the one hand, through experiments, it has been further validated that the superiority of adopting the proposed novel term “*tail quality*” can provide a more intuitive characterization of the severe consequences of instability in deep learning models and systems in real-world applications compared to relying solely on inference quality or inference time as evaluation metrics.

On the other hand, the experiments confirmed the effectiveness of this evaluation framework in predicting “tail quality.” During the testing phase, the evaluation framework achieved an average squared root of Jensen-Shannon Divergence (rJSD) value of 0.051 for the predicted probability distribution of inference times. Furthermore, in predicting the worst-case tail quality at the 99th, 95th, and 90th percentile tail latency thresholds, it exhibited an average discrepancy level of -0.07, indicating its ability to reasonably forecast the lower limit of tail quality’s worst-case scenario. In terms of the framework performance, MLPerf Inference [25] requires a minimum of 262,742 inferences to determine the 99th percentile

Tail Latency. In contrast, our proposed evaluation framework achieves a high level of prediction for tail quality, with an average of only 62.26% of these inferences across all experiments. Finally, a preliminary analysis of potential factors contributing to the occurrence of the “tail quality” phenomenon. Therefore, the authors urge caution in dealing with the discovered phenomenon of tail quality and call for establishing innovative methodologies and tools based on the proposed evaluation framework to tackle the challenge above.

2. Motivation

2.1. Why the metric of tail quality is essential?

Relying solely on inference quality or tail latency as metrics to assess the inference capability of deep learning is insufficient. Specifically, as depicted in Figure 1, an experiment is conducted using an image classification model ViT on a Tesla P100.

When there are no constraints on inference time, the deep learning model’s inference quality is 81.512%, with a 99th percentile tail latency of 472.41 ms. These two metrics are commonly employed in deep learning research: accuracy serves as an evaluation metric for model inference quality, while tail latency is used to gauge the stability of deep learning systems.

However, when tail quality is adopted as an evaluation metric and the inference time threshold is set to the 99th percentile tail latency (i.e., 99% tail quality @ 472.41 ms), the tail quality decreases from its original value of 81.512% to 79.80%, with fluctuations ranging between 79.80% and 81.14%. Moreover, setting the threshold at the 90th percentile tail latency leads to more pronounced fluctuations in tail quality (i.e., 90% tail quality @ 392 ms fluctuates from 68.26% to 76.78%).

These variations in inference quality due to inference time cannot be adequately captured solely by using traditional inference quality and tail latency metrics. Hence, utilizing tail quality as an evaluation metric is of paramount importance.

2.2. Why need a tail quality evaluation framework?

In critical tasks, the fluctuation in tail quality of deep learning inference at a specific threshold can significantly impact its practical applications. Lower tail quality values might lead to irreversible and severe consequences. For instance, in domains like autonomous driving or high-frequency trading systems, the constraints on inference time can be extremely stringent. In the event of inference failure, the consequences could involve loss of life and property. Hence, there’s a need to predict the phenomenon of tail quality and analyze its underlying causes.

However, constructing methods for prediction and analysis presents numerous challenges. On one hand, due to the complexity of deep learning and computer systems, modeling aspects such as inference quality, inference time, and the various components of deep learning proves to be highly difficult. On the other hand, owing to uncertainty of the inference time,

predicting tail quality might demand substantial computational overhead.

Therefore, the construction of accurate tail quality prediction and analysis models while keeping computational resource costs low is of paramount importance, yet it remains a challenging endeavor.

3. Tail Quality and Evaluation Framework

In order to proactively anticipate and prevent the occurrence of “tail quality,” this section will begin by providing its definition. This definition will serve as the foundation for the systematic construction of tail quality evaluation framework, enabling a scientifically grounded approach. Subsequently, an evaluation framework for “tail quality” will be introduced. This framework enables the prediction of potential future instances of tail quality in deep learning models with relatively low computational costs. Additionally, it facilitates the analysis of potential factors that influence the emergence of tail quality.

3.1. Definition of Tail Quality

During deep learning inference phase, given a dataset $D = \{x_i, y_i\}_{i=1}^n$ containing $n = |D|$ instances, model M reads input instances x_i from the dataset D , generating a set of inference results $Y' = \{y'_i\}_{i=1}^n$ where $y'_i = M(x_i)$. By comparing the difference between inference results Y' and the ground truth answers $Y = \{y_i\}_{i=1}^n$, inference quality Q of model M over the entire dataset D can be obtained. The calculation method of inference quality depends on the specific quality evaluation metric used, such as accuracy, AP, and F-score. Thus, the calculation process can be abstracted by using the metric calculation function q as shown below:

$$\begin{aligned} Q &= q(Y', Y) \\ &= q(\{M(x_i)\}_{i=1}^n, \{y_i\}_{i=1}^n). \end{aligned} \quad (1)$$

As shown in Equation 1, it is evident that when calculating inference quality, the inference result of each instance contributes to the overall inference quality Q accordingly. The specific contribution of each instance x_i can be abstracted into a contribution function c_i . Therefore, the quality Q can be further abstracted into the following formula:

$$\begin{aligned} Q &= q(\{x_i, y_i, M\}_{i=1}^n) \\ &= q(\{c_i(x_i, y_i, M)\}_{i=1}^n). \end{aligned} \quad (2)$$

In a specific task, assume the maximum allowable inference time is denoted as θ , which serves as the inference time threshold. The inference time taken by the model M on a particular instance x_i is denoted as $t_i(x_i, M)$. Thus, the following indicator function $\mathbf{1}_\theta$ can be used to determine the effectiveness of the inference result:

$$\mathbf{1}_\theta(x_i, M) = \begin{cases} 1 & t_i(x_i, M) \leq \theta, \\ 0 & t_i(x_i, M) > \theta. \end{cases} \quad (3)$$

Additionally, the instability of deep learning systems leads to constant fluctuations in model inference time. Thus, to better investigate the impact of inference time on inference quality, it can be assumed that the inference time $t_i(x_i, M)$ of model M on instance x_i follows a certain conditional probability distribution

$$P(T = t \mid \mathcal{X} = x_i, \mathcal{M} = M) \quad (4)$$

where T , \mathcal{X} , and \mathcal{M} are three random variables representing time, instance, and model, respectively. $t_i(x_i, M)$ is replaced by t to make the expression more concise. Note that the specific model is already determined during the deep learning inference phase.

Ultimately, under the constraint of inference time, the overall inference quality Q can be represented as the following equation:

$$Q = q(\{c_i(x_i, y_i, M) \cdot \mathbf{1}_\theta(x_i, M)\}_{i=1}^n). \quad (5)$$

Based on the formulas provided above, it becomes evident that once deterministic inference quality algorithm is now reliant on the inference time of each instance, introducing considerable uncertainty in the calculation inference quality due to considering inference time constraints.

Note that the above analysis applies when the input is a batch; the probability distribution and indicator function corresponding to each instance in the batch can be simply replaced by the ones corresponding to the entire batch.

3.2. Establishment of Evaluation Framework

The systems, models, data, and other components influence the deep learning inference time, which, in turn, indirectly affects the deep learning inference quality and causes fluctuations in the inference quality. This section introduces a novel evaluation framework based on the definition of the ‘‘tail quality’’ phenomenon. The framework aims to accurately predict and provide a systematic approach for assessing and understanding this phenomenon. The framework models the entire evaluation process from the system, model, data, and other potential components to the inference time and then to the inference quality, based on the definition of ‘‘tail quality’’ from the previous subsection. It allows researchers to adjust the modeling formulas and parameters to guide the establishment of evaluation processes with varying levels of granularity and precision. This provides the evaluation framework with high flexibility and scalability.

Taking into account the correlation between deep learning inference and components that researchers care about, such as the data, model, deep learning framework, operating system, and system architecture, the variation of each component can potentially impact the probability distribution of the deep learning inference time. Therefore, the probability distribution model that describes and analyzes the various influencing factors that impact the inference time of deep learning can

be represented as the conditional probability distribution of inference time, as shown below:

$$P(T \mid \mathcal{C}^1, \mathcal{C}^2, \dots), \quad (6)$$

where \mathcal{C}^j denotes the influencing components.

In a practical application of the framework, components that are not considered or not listed will not appear in the distribution. Therefore, to ensure the objectivity of the analysis, the evaluation environment for deep learning inference should remain unchanged except for the listed components. The more components \mathcal{C}^j are listed, the more factors are considered by researchers. However, it also means that more control variables need to be considered, making the analysis more complex and cumbersome. Equation 4 is an instantiation of the distribution model 6, where only the deep learning model \mathcal{M} and data \mathcal{X} components are considered, and it is assumed that the other components remain unchanged during the formula derivation. Adding more components to this model will not affect the results of the derivation of this section.

Building on this inference time distribution model, the inference quality represented by Formula 5 can be rewritten to create the model that describes and analyzes the impact of inference time on inference quality, as shown below:

$$Q = q(\{c_i(x_i, y_i, M) \cdot \mathbf{1}_\theta(x_i, M, \{\mathcal{C}^j\}_{j=1}^\infty)\}_{i=1}^n) \quad (7)$$

where the characteristic function $\mathbf{1}_\theta(x_i, M, \{\mathcal{C}^j\}_{j=1}^\infty)$ is rewritten to be as:

$$\mathbf{1}_\theta(x_i, M, \{\mathcal{C}^j\}_{j=1}^\infty) = \begin{cases} 1 & t_i(x_i, M, \{\mathcal{C}^j\}_{j=1}^\infty) \leq \theta, \\ 0 & t_i(x_i, M, \{\mathcal{C}^j\}_{j=1}^\infty) > \theta, \end{cases} \quad (8)$$

where $t_i(x_i, M, \{\mathcal{C}^j\}_{j=1}^\infty)$ follows the distribution 6.

With the formulation of Formula 6, 7, and 8, the model of the evaluation framework has been established. Therefore, the construction of the evaluation framework mainly consists of two parts: (1) establishing a probability distribution model for inference time, as shown in Equation 6, through which the relationship between individual components and inference time can be determined; (2) constructing a ‘‘tail quality’’ calculation model to establish the mapping relationship between inference quality and inference time through this model, as Equation 7 represents.

Inference Time Probability Model

In this section, a heuristic algorithm is proposed to estimate the probability distribution of inference times, which can be seen as a basic Monte Carlo simulation. As the probability distribution governing the inference time of each instance is unknown, this part proposes a heuristic algorithm to estimate the probability distribution of inference time, in order to construct the inference time probability model. This estimation process can be viewed as a fundamental Monte Carlo simulation.

Algorithm 1 shows details of the proposed algorithm. Initially, the deep learning model M conducted r rounds of inference for all instances x_i in the dataset D where $|D| = n$,

Algorithm 1 Estimation of Inference Time Analysis Model

Input: $M, \{x_i\}_{i=1}^n, n, r, s, \delta,$ and w **Output:** $r, \{f_i\}_{i=1}^n,$ and $\{\hat{y}_i\}_{i=1}^n$

```
1: // Initialization
2: for all  $i \leftarrow 1 \dots n$  do
3:   for all  $j \leftarrow 1 \dots r$  do
4:      $t_{i,j} \leftarrow \text{Timing}(M(x_i))$ 
5:   end for
6:    $\hat{y}_i \leftarrow M(x_i)$ 
7:    $F_{i,1} \leftarrow \text{Fit}(\{t_{i,j}\}_{j=1}^r)$ 
8: end for
9:
10: // Iteration
11:  $l \leftarrow 1$ 
12: repeat
13:    $r \leftarrow r + l$ 
14:   for all  $i \leftarrow 1 \dots n$  do
15:      $t_{i,j} \leftarrow \text{Timing}(M(x_i))$ 
16:     if  $l \bmod s = 0$  and  $fit_i \neq \text{True}$  then
17:        $F_{i,l+1} \leftarrow \text{Fit}(\{t_{i,j}\}_{j=1}^r)$ 
18:        $f_i \leftarrow F_{i,l+1}$ 
19:       if  $l + 1 > w$  then
20:         for all  $k \leftarrow l + 1 - w \dots l$  do
21:            $fit_k \leftarrow \text{True}$ 
22:           if  $\text{Check}(F_{i,k}, F_{i,l+1}) > \delta$  then
23:              $fit_k \leftarrow \text{False}$ 
24:           end if
25:         end for
26:       end if
27:     end if
28:   end for
29:    $finish \leftarrow \text{True}$ 
30:   for all  $i \leftarrow 1 \dots n$  do
31:     if  $fit_i \neq \text{True}$  then
32:        $finish \leftarrow \text{False}$ 
33:     end if
34:   end for
35:    $l \leftarrow l + 1$ 
36: until  $finish = \text{True}$ 
```

recording the corresponding inference times, and then, by using the method $\text{Fit}()$, the probability density functions (PDF) for each instance are fitted based on the initial recorded r rounds of inference times (line 2-8). Researchers can opt for an appropriate function-fitting method to model the probability distribution of inference times for each instance. In this study, the kernel density estimation (KDE) method is chosen to employ. According to the definition of KDE, the fitted PDF of the instance x_i is as follows:

$$f_i(t) = \text{Fit}(\{t_{i,j}\}_{j=1}^r) = \frac{1}{nh} \sum_{j=1}^r K\left(\frac{t-t_{i,j}}{h}\right), \quad (9)$$

where $t_{i,j}$ is the j th round inference time on the instance x_i , K is the kernel function which is chosen as a Gaussian distribution

in the paper, and h is a smoothing parameter.

The algorithm then proceeds to perform deep learning inference on the entire dataset repeatedly until it deems that the PDF for all instances has been sufficiently well-fitted (lines 12-36). Firstly, during each inference, the inference times on all instances are recorded (line 15). Then, on the entire dataset, for every s rounds of inference, the probability distribution models for the inference times of all instances are re-fitted based on the newly recorded s inference times as well as all the previously recorded inference times (line 16, 17). The newly fitted model $F_{i,l+1}$ is then compared with the previously fitted models.

With an increase in the number of inference rounds, the accumulation of more recorded inference times yields additional information about the population of inference times. This enables a more accurate estimation and prediction of probability distribution. Therefore, when newly recorded inference times cease to contribute information significantly to the estimation of the probability distribution, indicating that the fitting of the distribution hardly changes, it is considered that a reasonably good estimation of the overall distribution has been achieved.

Based on these considerations, Algorithm 1 employs a sliding window to store the previous w fitted distributions. If the differences between these fitted distributions within the sliding window are sufficiently small, i.e., they are less than the specified tolerance threshold δ , it is inferred that a sufficiently good estimation of the statistical population can be obtained based on the available inference time records (line 20-25).

The algorithm employs the $\text{Check}()$ method to compare differences among different fitting results (line 22). This method can be specified by researchers as long as it ensures the convergence of the algorithm is not compromised. In this paper, the $\text{Check}()$ method employs Jensen-Shannon (JS) divergence, which is a symmetrized and smoothed version of the Kullback-Leibler (KL) divergence, to quantify the similarity between any two probability distributions. The definition of the JS divergence is:

$$\text{JSD}(P \parallel Q) = \frac{D(P \parallel M) + D(Q \parallel M)}{2}, \quad (10)$$

where P and Q are the probability distributions to be compared, they correspond to $F_{i,k}$ and $F_{i,l+1}$ respectively in the context of Algorithm 1, and $M = \frac{1}{2}(P + Q)$ represents the mixture distribution of P and Q . $D(P \parallel Q)$ denotes the calculation of the KL divergence between P and Q .

Ultimately, after finishing the estimation of the inference time distribution for all instances, it can be inferred that the fitted probability density functions $f_{i=1}^n$ of each instance and the minimum required number of inference rounds to obtain these density functions. The computation cost of this algorithm mainly depends on the number of iterations needed to fit PDFs of inference times for all samples. Consequently, the total number of inferences should be the product of the dataset size and the number of iterations. Through experi-

ments in Section 4, it can be observed that the algorithm’s fitting convergence rate is quite satisfactory and, in most cases, it outperforms the inference count required by MLPerf Inference [25].

Tail Quality Calculation Model

As evident from the previous sections, deriving an analysis model for inference quality directly from the inference time analysis model through Formula 7 is quite challenging. Given the variety of evaluation metrics, it is not feasible to construct quality calculation functions for each metric and to estimate the contribution functions of all instances under specific quality indicators.

Fortunately, the process of estimating the inference time distribution model involves a comprehensive exploration of all potential deep learning inference conditions that may occur. Hence, given all the recorded inference times, researchers can easily calculate the inference quality for each round of inference at a specific threshold θ by utilizing Algorithm 2, which is derived from the Equations 7 and 8.

In Algorithm 2, the inference result effectiveness of each instance is tagged by comparing its inference time with the threshold θ (line 4-8). Deep learning inference results that surpass the inference time threshold will be marked as invalid and considered as erroneous outcomes in the overall statistical evaluation of inference quality. After each round of tagging is completed, the inference quality can be recalculated by using method Evaluate() based on the effectiveness of all instances in the dataset (line 10). Implementing the Evaluate() method depends on a specific inference quality metric. For instance, in the case of accuracy evaluation metric, all invalid instances (i.e., instances where $v_j = False$) can be considered as errors when assessing correctness against the ground truth. This means they are not included in the count of correct samples, while other valid instances are counted according to the original calculation method.

Finally, with the calculated qualities through Algorithm 2, researchers can directly estimate the probability distribution of the inference quality under the specified inference time threshold θ , which makes the inference quality analysis model more concrete. However, in practical applications, estimating this distribution model is not always necessary. The emphasis should lie on particular attributes crucial for real-world applications, such as the worst-case quality at the 99th percentile tail latency threshold and the 99th percentile tail quality at a designated threshold.

4. Experimental Analysis and Results

In this section, the authors first instantiate the proposed evaluation framework and validate its effectiveness through experiments. Subsequently, the instantiated evaluation framework is employed to analyze various factors, such as systems and data, that impact inference time and inference quality separately.

Algorithm 2 Calculation of Inference Quality

Input: $M, r, \theta, \{x_i, y_i\}_{i=1}^n, \{\hat{y}_i\}_{i=1}^n, \{t_{i,j}\} (i \in [1, n], j \in [1, r])$
Output: Inference Qualities $\{q_i\}_{i=1}^r$

```

1:
2: for all  $i \leftarrow 1 \dots r$  do
3:   for all  $j \leftarrow 1 \dots n$  do
4:     if  $t_{j,i} \leq \theta$  then
5:        $v_j \leftarrow True$ 
6:     else
7:        $v_j \leftarrow False$ 
8:     end if
9:   end for
10:   $q_i \leftarrow Evaluate(\{x_j, \hat{y}_j, v_j\}_{j=1}^n)$ 
11: end for

```

4.1. Instantiation of the Evaluation Framework

The instantiation of the evaluation framework essentially involves defining the analysis models for inference time and inference quality and selecting appropriate parameters for the estimation Algorithms 1 and 2. For the sake of experiments simplicity, this study considers four influencing factors: hardware systems \mathcal{S} , deep learning frameworks \mathcal{F} , models \mathcal{M} , and data \mathcal{X} . Equation 6 is then given as follows:

$$P(T | \mathcal{X}, \mathcal{M}, \mathcal{S}, \mathcal{F}). \quad (11)$$

To define the search space for influencing components, four servers are selected with different types of graphics processing units (GPU) as subjects for hardware systems \mathcal{S} investigation in experiments. Among them, Server A is equipped with 4 identical GeForce RTX 2080 Ti GPUs, facilitating distributed inference for large language models (LLM). For deep learning frameworks \mathcal{F} , experiments are conducted under the two most popular frameworks, PyTorch [23] and TensorFlow [1]. Noting that the framework versions are consistent across all servers, and the CUDA version is 11.7 for all except Server C. The detailed configurations are presented in Table 1

In order to ensure comprehensiveness while maintaining simplicity in experiments, for models \mathcal{M} and data \mathcal{X} inference components, three widely used models were selected across the Computer Vision (CV) and Natural Language Processing (NLP) domains. These models include Detection Transformer (DETR) [2] for object detection, Vision Transformer (ViT) [7] for image classification, and the large language model Vicuna [38] for dialogue systems (Chatbot). Except for Vicuna, which is implemented solely using the official PyTorch implementation, the other two models have both their official implementations and equivalent implementations in the other framework. Corresponding to the selected models, three datasets used to evaluate the model inference quality, namely COCO [20] val2017, ImageNet [26] val2012, and MMLU [17] dev, were chosen for conducting the experiments. Furthermore, due to the limitation that DETR only supports an input batch size of 1, a variant of the DETR model, namely DETR-DC5,

Table 1: Detailed System Configurations

Specs		Server A	Server B	Server C	Server D
GPU	Type	GeForce RTX 2080 Ti	TITAN V	Tesla P100	Tesla V100
	Cores	4352	5152	3584	5120
	Memory	11GB	12GB	16GB	32GB
	Amount	4	1	1	1
	Architecture	Turing	Volta	Pascal	Volta
	CUDA Version	11.7	11.7	11.6	11.7
PyTorch		1.12.1			
TensorFlow		2.13.0			
CPU		Intel(R) Xeon(R) CPU E5-2620 v3 @ 2.40G			

Table 2: Tasks, corresponding models, data sets, and inference quality evaluation metrics used in the fields of Computer Vision(CV) and Natural Language Processing(NLP) in experiments. The numbers placed in parentheses below the dataset names and model names represent the number of instances in dataset and the number of model parameters, respectively. In these annotations, ‘K’, ‘M’, and ‘B’ respectively denote ‘thousand’, ‘million’, and ‘billion’. ‘mAP’ and ‘Acc’ respectively denote mean Average Precision and Accuracy.

Area	Task	Model	Data Set	Metric
CV	Object Detection	DETR ($\approx 60M$)	COCO (5K)	mAP
CV	Image Classification	ViT ($\approx 306M$)	ImageNet (50K)	Acc
NLP	Dialogue System	Vicuna ($\approx 13B$)	MMLU (1531)	Acc

is utilized for experiments with a batch size of 2. Both models have the same number of parameters. As shown in Table 3, experiments with the ViT and DETR models are conducted solely on Servers A, B, and C. On the other hand, experiments with the Vicuna model are conducted solely on Servers A and D. Table 2 contains specific information about the data and models.

Another part of the framework instantiation involves selecting hyperparameters for the estimation Algorithm 1 of the inference time probability model. Specifically, the initial number r of inference rounds is set to 30, the size of sliding window w for storing fitted analysis models is set to 5, and the step size s for re-fitting is set to 5. The tolerance δ for similarity differences between the fitted models is set to 0.2. It’s important to note that the evaluation metric for tolerance difference is the square root of Jensen-Shannon Divergence (rJSD). JSD ranges from 0 to 1, where lower values indicate more remarkable similarity between two fitted results, with 0 representing identical.

4.2. Validation of Effectiveness

To validate the effectiveness of the evaluation framework, the validation process is divided into two stages: the training and testing stages.

In training stage, inference time probability models are es-

timated on different servers and deep learning frameworks for each model and its corresponding dataset. A probability density distribution (PDF) is fitted for each instance based on its inference times. The fitted PDF should stabilize as the algorithm iterates, indicating that the rJSD between the re-fitted PDF and the existing w PDFs, which were fitted using a smaller amount of inference time data, should gradually approach 0. Therefore, rJSD serves as a metric to assess the quality of the fitting results for each instance. Furthermore, the mean rJSD across all instances in the dataset is employed as an indicator of the overall quality of the algorithm in fitting the entire dataset.

In testing phase, to assess the generalization performance of PDF of inference times corresponding to each fitted instance by the algorithm, all deep learning models undergo an additional 30 rounds of inference on their respective datasets. This process generated new inference time data points, which were then used to validate the generalization performance of the probability distributions that are fitted during the training phase. A better generalization performance indicates that the fitting results encompass sufficient information about the population, capturing a broader range of scenarios that deep learning models might encounter during repeated inferences on the same instance. Specifically, during the testing phase, probability distribution are fitted to all the inference time data obtained for each instance in the dataset. Subsequently, the fitted results obtained for each sample during the training phase are individually compared with the corresponding testing phase results, and the rJSD is calculated for each comparison. The overall generalization performance of the estimated inference time probability model across the whole dataset can be represented by the average rJSD computed for all instances.

The validation of the tail quality calculation model can be conducted by comparing the statistical metrics of the predicted tail quality by the calculation model with the difference in tail quality observed during the testing phase.

Fitting Quality and Generalization Performance

Table 3 presents the fitting quality of inference time probability models obtained from the training phase for all deep learning models across various servers and frameworks, as well as the generalization performance of the probability models in the

Table 3: Square root of Jensen-Shannon divergence (rJSD) of all inference time analysis models corresponding to different deep learning models in the training and testing stage, with rJSD approaching 0 indicating that the fitting results are closer to the statistical population. Note that all rJSD results in the table are the average values of the entire dataset. For specific configurations of all servers, refer to Table 1. N/A signifies the absence of relevant experiments.

Model	Batch Size	Framework	Server A		Server B		Server C		Server D	
			Train	Test	Train	Test	Train	Test	Train	Test
DETR (DC5)	1	PyTorch	0.000	0.004	0.002	0.036	0.000	0.007	N/A	N/A
		TensorFlow	0.032	0.204	0.025	0.155	0.010	0.190	N/A	N/A
DETR	2	PyTorch	0.000	0.004	0.001	0.011	0.015	0.207	N/A	N/A
		TensorFlow	0.030	0.214	0.018	0.154	0.006	0.011	N/A	N/A
ViT	256	PyTorch	0.001	0.011	0.001	0.013	0.001	0.015	N/A	N/A
		TensorFlow	0.011	0.195	0.006	0.127	0.009	0.206	N/A	N/A
Vicuna	1	PyTorch	0.006	0.111	N/A	N/A	N/A	N/A	0.000	0.007

testing phase. It is evident that all the JSD values, which are the squares of the rJSD values in the table, are below 0.05. This indicates that the evaluation framework can effectively fit the probability distribution of inference times for each instance when estimating the inference time probability models for the influencing components. Furthermore, each probability model demonstrates strong generalization on new data, indicating that the model comprehensively captures various scenarios during the deep learning inference process. One reason for some test rJSD values being larger than their corresponding training phase values is that the testing phase involves fewer data points for fitting the probability density function. Consequently, the fitting process during the testing phase lacks a significant amount of crucial information compared to the training phase, leading to discrepancies in the fitting results between the two phases.

Characterization of Tail Quality

Furthermore, to ascertain whether the tail quality calculation model can be derived by constructing the inference time probability model within the proposed evaluation framework, specific thresholds were employed to assess the inference quality of deep learning models in both the training and testing phases. By contrasting the differences in statistical indicators of these inference quality measurements, it is possible to preliminarily determine if the tail quality calculation model possesses certain statistical characteristics. The experiments employ tail latencies from 3 distinct percentiles - specifically, the 99th, 95th, and 90th percentiles of all inference times - as thresholds for computing tail quality. Subsequently, the worst-case tail quality values is determined to observe the ability of prediction for tail quality in testing stage of the calculation model. As illustrated in the Table 4, the differences between training and testing stage in worst-case tail quality among all models on Server A are almost all below 0. This suggests that the tail quality calculation model has achieved favorable estimations through the inference time probability model, and the value of the worst-case tail quality has been accurately predicted. Furthermore, by examining the statistics of different $x\%$ tail quality in the table, it is evident that the calculation models

effectively capture the tail quality phenomena at various inference time thresholds. As the thresholds become stricter, the worst-case tail quality gradually decreases. This further validates the significance of tail quality, and the efficacy of this evaluation framework in predicting tail quality.

Efficiency of the Evaluation Framework

Due to the adoption of the heuristic algorithm for estimating the evaluation model, the computational resource expenditure in constructing this model depends on the number of iterations the algorithm takes to converge and the size of the dataset. Table provides an account of the total inference count required for estimating the analysis model across all experiments. This total inference count pertains to the fitting of PDF for inference times across all instances, rather than referring to inference rounds conducted on the entire dataset. MLPerf Inference [25] stipulates that a total of 270,336 inferences should be conducted to statistically capture the 99th percentile tail latency. As evident from the Table 5, the inference counts in all experiments are below this value except the model DETR-DC5. The evaluation framework’s average number of inference iterations across all models, compared to MLPerf, resulted in approximately 37.74% reduction in computational workload. Consequently, the computational resource expenditure of this evaluation framework is manageable in practical applications.

4.3. Analysis of Influencing Components

After validating the effectiveness of the evaluation framework, this section will employ the instantiated framework to conduct a comprehensive analysis of the individual components that impact both inference time and inference quality. For the sake of conciseness and focused attention, this section primarily delves into the specific analysis of experiments related to the DETR-DC5 model in object detection tasks. Henceforth, DETR will be used directly to refer to the DETR-DC5 model. Where necessary, additional analyses of other experiments will also be incorporated.

Effect of the Input Data

Impact of different instance sizes on inference time: Due to the characteristics of the DETR model and the nature of the

Table 4: The worst-case $X\%$ tail quality of different models on Server A during both the training and testing phases, where X represents the percentile of tail latency used as the threshold. The values in the column with the Δ symbol represent the difference between the worst-case $X\%$ tail quality during the training and testing stages. A smaller difference indicates that the evaluation framework predictions for the worst-case scenario are better.

Model	Framework	99% Tail Quality			95% Tail Quality			90% Tail Quality			Origin Quality
		Train	Test	Δ	Train	Test	Δ	Train	Test	Δ	
DETR (DC5)	PyTorch	43.93	44.29	-0.36	41.72	42.35	-0.62	39.47	40.03	-0.56	44.90
	TensorFlow	44.11	44.18	-0.07	41.90	42.20	-0.30	39.21	39.45	-0.24	44.80
DETR	PyTorch	43.03	43.04	-0.02	41.10	41.12	-0.03	39.00	39.16	-0.16	43.50
	TensorFlow	42.57	42.79	-0.22	40.16	40.32	-0.16	37.16	37.69	-0.54	43.40
ViT	PyTorch	78.53	76.72	1.81	65.36	68.64	-3.29	48.00	53.65	-5.65	81.51
	TensorFlow	79.29	79.73	-0.44	70.18	72.31	-2.13	63.76	65.62	-1.87	81.51
LLM	PyTorch	51.99	51.99	0.00	50.23	50.16	0.07	48.47	48.47	0.00	52.71

Table 5: The total inference count of evaluation framework required for constructing the tail quality prediction model across various models and systems. The percentage under the average value represents the ratio of its inference count to that of MLPerf Inference. N/A signifies the absence of relevant experiments.

Model	Framework	Server A	Server B	Server C	Server D	MLPerf
DETR (DC5)	PyTorch	350,000	350000	350,000	N/A	262,742
	TensorFlow	350,000	350000	350,000	N/A	262,742
DETR	PyTorch	175,000	175000	175,000	N/A	262,742
	TensorFlow	175,000	175000	175,000	N/A	262,742
ViT	PyTorch	13,720	13720	13,720	N/A	262,742
	TensorFlow	13,720	13720	13,720	N/A	262,742
LLM	PyTorch	107,170	N/A	N/A	107,170	262,742
Average Inference Count		169,230 (64.41%)	179,573 (68.35%)	179,573 (68.35%)	107,170 (40.79%)	262,742 (100%)

object detection task, instances of the dataset isn't uniformly cropped to the same size before being fed into the model for inference. Therefore, it is reasonable to assume that the inference time of the model may be influenced by the size of the input data, indicating a potential correlation between the two. To validate this hypothesis, experiments conducted linear regression about the DETR model, examining the relationship between the number of pixels of input images and the time taken for inference on different deep learning frameworks and servers. As depicted in Figure 3 (a) and (b), across all servers and regardless of whether TensorFlow or PyTorch is chosen as the deep learning framework, the model's inference time exhibits a positive linear correlation with the image size.

This confirms the hypothesis that as the image size increases, the computational workload of the deep learning system during inference also increases, subsequently leading to longer inference times. Therefore, if the aim is to reduce model inference time, exploring solutions from the perspective of compressing image sizes could be a viable approach. A similar phenomenon is observed in dialogue systems as well. For chatbots like Vicuna, the inputs consist of sentences of varying lengths, also known as prompts, where the length is determined by the number of tokens after sentence segmentation. In human-machine dialog scenarios, the input length during each model inference is highly likely to be different. There-

fore, as depicted in Figure 3 (c), the length of input sentences shows a positive linear correlation with the inference time of Vicuna.

Impact of same instance sizes on inference time: Interestingly, as evidenced by the scatter plot in Figure 3 (a) and (b), even when the image pixel count remains consistent and inferences are conducted on the same system, DETR model still exhibits significant fluctuations in inference time for different input samples. To analyze the underlying reasons for these discrepancies, experiments compared the frequency distributions of inference times for different images of the same size. As shown in Figure 2, even though images #4159, #3961, and #17 share the same dimensions, their frequency distributions for inference times still exhibit notable differences. One possible reason for this phenomenon might be linked to the sparsity of images. Furthermore, an insightful observation is that when categorizing images of the same size based on their width and height, it becomes apparent that images with longer heights tend to have relatively longer inference times. Unfortunately, due to space constraints, the detailed analysis data is not presented here. For a more comprehensive analysis, a finer-grained segmentation of the conditional random variables within the evaluation framework would be necessary.

Sensitivity of inference time analysis model to variations in input data: It's evident that input data indeed impact the

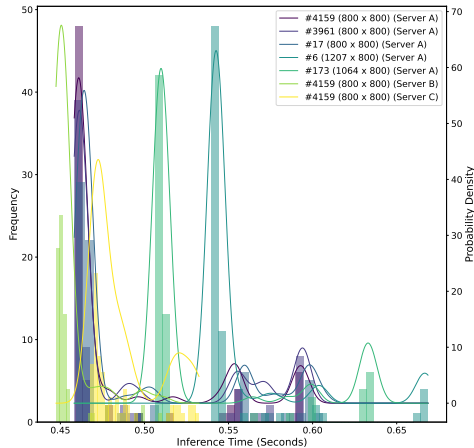


Figure 2: Fitting of probability density functions for inference times of instances with varying sizes, as well as for instances of the same size on different systems. The histograms represent the frequencies of instance inference times, with values corresponding to the left y axis. The curves illustrate the fitted probability density curves based on instance inference times, with values corresponding to the right y axis. This figure displays experimental results for five randomly selected distinct samples from the dataset, encompassing three different sizes and three distinct servers.

model’s inference time, though the differences in the effects generated by many instances are not excessively significant. An effective evaluation framework should exhibit sensitivity to subtle discrepancies and adeptly capture these differences, allowing for the differentiation of various analysis models. As inference time is positively correlated with input instance size, its distribution of statistical population should also exhibit a positive correlation with input size. Figure 4 highlights that the evaluation framework’s fitting of inference time distribution across different input data sizes nearly aligns with a positive correlation relationship. Furthermore, as observed in Figure 2, the evaluation framework also performs well in fitting models with very small distinctions in inference time frequency distribution. Notably, the differences in the fitted curves corresponding to three images of the same size are clearly discernible.

Effect of the Hardware and Software Systems

In addition to the analysis of input data, the instantiated evaluation framework also takes into account the influence of deep learning frameworks \mathcal{F} and systems \mathcal{S} on the inference results. As the search space for \mathcal{F} and \mathcal{S} is significantly smaller than that of input data, this aspect of the analysis is relatively straightforward. Of course, as granularity increases for the division of frameworks and systems, the complexity of analysis will increase along with the expansion of the search space. However, it’s worth noting that these considerations are beyond the scope of this work.

As evident from Figure 3 in the experiments with the DETR model, regardless of the framework used, Server C (Tesla V100) consistently exhibits shorter inference times compared

to the other two servers. Conversely, Server C (GeForce RTX 2080 Ti) notably performs worse than the other two servers, and its rate of increase in inference time with respect to increasing image size (slope of the regression line) is slower than that of the other servers. This can also be observed from the fitting results of the inference time distribution for image #4159 across different servers, as depicted in Figure 2. Also, the inference speed of PyTorch is notably higher than that of TensorFlow. Furthermore, due to Vicuna’s extensive parameter count of 13 billion, it necessitates the utilization of 4 GPUs for distributed model inference on Server A. As depicted in the Figure 3, the inference time on Server A remains considerably longer than that on Server C. This can be attributed to a combination of factors, including GPU performance differences and the impact of data communication speed among GPUs during distributed inference.

5. Related Work

Numerous works study inference quality and inference time of deep learning models and systems in real-world applications. Hence, this section elucidates the distinction between this research and other related works to establish its unique contributions.

5.1. Optimization of Inference Quality and Time

Domain generalization aims to address the issue of significant inference quality degradation that may occur in well-trained deep learning models when facing unseen domains [31, 39]. In contrast, our research primarily focuses on the phenomenon called tail quality, where the inference quality of deep learning models may fluctuate and experience a substantial decline when processing the same data.

Efficient neural network inference primarily focuses on increasing the computational efficiency of models under resource constraints, employing solutions like model quantization and model pruning, which often entail alteration of the original model [12, 13, 15, 18]. However, our work primarily concerns identifying inefficient inference processes and analyzing the underlying causes while keeping the model intact.

5.2. Benchmarking of Deep Learning Inference

Evaluation of deep learning models primarily focuses on specific inference quality metrics. For instance, *Average Precision (AP)* is the most popular metric that is used in various benchmark challenges for object detection, such as Pascal VOC [8] and MS COCO [20]. *Accuracy* and *F-score* are utilized to evaluate most state-of-the-art classification models, such as large language models in the field of natural language processing [6, 38] and image classification models in autonomous driving, emotion recognition and healthcare [22, 24, 29, 35, 37]. Using only inference quality metrics can only reflect the optimal predictive ability of models on a specific test dataset. Although, in addition to quality metrics, many studies also employ other system-related metrics to evaluate the processing

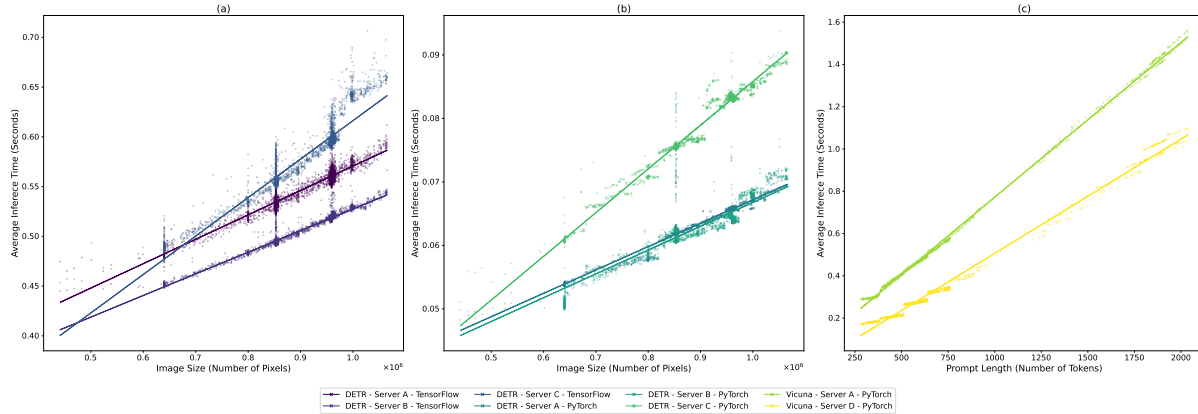


Figure 3: The relationship between the size of the instances of the dataset (COCO and MMLU) and the corresponding average inference time, which is established using linear regression. Sub-figures (a) and (b) present experimental results for the DETR model implemented in TensorFlow and PyTorch on three different servers, A, B, and C, respectively. Sub-figure (c) illustrates the experimental results for the Vicuna model implemented in the PyTorch framework on two different servers, A and D.

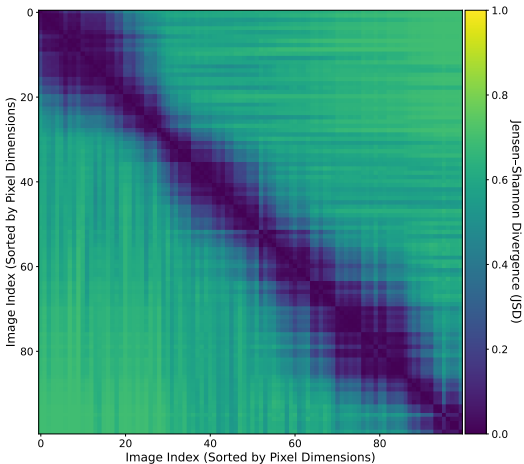


Figure 4: The Jensen-Shannon Divergence (JSD) between the probability density distributions of inference times fitted for each instance is depicted. The recorded inference times are derived from experiments conducted on the DETR model in the context of object detection tasks using the COCO dataset. Both x and y axes of the heatmap are sorted in ascending order according to the size of the images, sorted by the number of pixels. Due to limitations in dataset size, this heatmap displays only 100 instances with distinct sizes present in the dataset.

speed of models [29], such as *floating-point operations per second (FLOPS)* [7, 28] and *frames per second (FPS)* [21], the impact of changes in deep learning systems on inference quality and time are not taken into account. These inference time metrics, such as FLOPS and FPS, can only reflect the average inference efficiency of the model on specific deep learning software and hardware systems. When processing samples, they cannot illustrate how poorly models perform on different software and hardware systems.

Benchmarking of deep learning systems tends to prioritize

inference time, throughput, and other system-related metrics. MLPerf Inference [25] and AIBench [9, 10], for example, utilizes *tail latency* as its evaluation metric, while DAWN-Bench [4] adopts *average inference latency*. Although tail latency can reflect the stability and reliability of deep learning systems [5, 25], helping identify issues for performance optimization, it cannot directly reflect the impact of variability and performance issues of systems on inference quality, as well as the potential adverse consequences may rise. Indeed, these benchmark suites also incorporate inference quality as part of the evaluation procedure. Still, it is primarily used to set specific inference quality targets to ensure that the workloads meet the conditions imposed as benchmarks and is sufficient to assist in measuring the inference time consumed by different systems.

6. Conclusion

This paper unveils a counterintuitive phenomenon, where in the practical application of deep learning inference, there are fluctuations in inference quality. Existing evaluation metrics fail to intuitively depict these quality fluctuations and their worst inference performance. To address this, a novel metric called "tail quality" is introduced in this paper to characterize this phenomenon. Due to the potential severe consequences of tail quality, such as loss of life or property damage, effective prediction and comprehensive analysis of tail quality are crucial. To tackle this issue, a flexible and scalable tail quality evaluation framework is proposed, which can make reasonably accurate predictions of tail quality with lower computational costs than the state-of-the-art like MLPerf Inference. In conclusion, the authors aim to draw attention to the phenomenon depicted by "tail quality" and call for exploration of more comprehensive evaluation methods based on the proposed evaluation framework in this paper.

References

- [1] Martín Abadi, Paul Barham, Jianmin Chen, Zhifeng Chen, Andy Davis, Jeffrey Dean, Matthieu Devin, Sanjay Ghemawat, Geoffrey Irving, Michael Isard, Manjunath Kudlur, Josh Levenberg, Rajat Monga, Sherry Moore, Derek G. Murray, Benoit Steiner, Paul Tucker, Vijay Vasudevan, Pete Warden, Martin Wicke, Yuan Yu, and Xiaoqiang Zheng. TensorFlow: A system for large-scale machine learning. In *Proceedings of the 12th USENIX Conference on Operating Systems Design and Implementation*, OSDI'16, pages 265–283, USA, November 2016. USENIX Association. ISBN 978-1-931971-33-1.
- [2] Nicolas Carion, Francisco Massa, Gabriel Synnaeve, Nicolas Usunier, Alexander Kirillov, and Sergey Zagoruyko. End-to-End Object Detection with Transformers. In Andrea Vedaldi, Horst Bischof, Thomas Brox, and Jan-Michael Frahm, editors, *Computer Vision – ECCV 2020*, Lecture Notes in Computer Science, pages 213–229, Cham, 2020. Springer International Publishing. ISBN 978-3-030-58452-8. doi: 10.1007/978-3-030-58452-8_13.
- [3] Chenyi Chen, Ari Seff, Alain Kornhauser, and Jianxiong Xiao. DeepDriving: Learning Affordance for Direct Perception in Autonomous Driving. In *2015 IEEE International Conference on Computer Vision (ICCV)*, pages 2722–2730, December 2015. doi: 10.1109/ICCV.2015.312.
- [4] Cody Coleman, Deepak Narayanan, Daniel Kang, Tian Zhao, Jian Zhang, Luigi Nardi, Peter Bailis, Kunle Olukotun, Chris Ré, and Matei Zaharia. DAWN-Bench: An End-to-End Deep Learning Benchmark and Competition. In *Workshop on ML Systems at Advances in Neural Information Processing Systems*, 2017.
- [5] Jeffrey Dean and Luiz André Barroso. The tail at scale. *Communications of the ACM*, 56(2):74–80, February 2013. ISSN 0001-0782. doi: 10.1145/2408776.2408794. URL <https://dl.acm.org/doi/10.1145/2408776.2408794>.
- [6] Jacob Devlin, Ming-Wei Chang, Kenton Lee, and Kristina Toutanova. BERT: Pre-training of Deep Bidirectional Transformers for Language Understanding. In *Proceedings of the 2019 Conference of the North American Chapter of the Association for Computational Linguistics: Human Language Technologies, Volume 1 (Long and Short Papers)*, pages 4171–4186, Minneapolis, Minnesota, June 2019. Association for Computational Linguistics. doi: 10.18653/v1/N19-1423. URL <https://aclanthology.org/N19-1423>.
- [7] Alexey Dosovitskiy, Lucas Beyer, Alexander Kolesnikov, Dirk Weissenborn, Xiaohua Zhai, Thomas Unterthiner, Mostafa Dehghani, Matthias Minderer, Georg Heigold, Sylvain Gelly, Jakob Uszkoreit, and Neil Houlsby. An Image is Worth 16x16 Words: Transformers for Image Recognition at Scale. In *International Conference on Learning Representations*, April 2023. URL <https://openreview.net/forum?id=YicbFdNTTy>.
- [8] Mark Everingham, Luc Van Gool, Christopher K. I. Williams, John Winn, and Andrew Zisserman. The Pascal Visual Object Classes (VOC) Challenge. *International Journal of Computer Vision*, 88(2):303–338, June 2010. ISSN 1573-1405. doi: 10.1007/s11263-009-0275-4. URL <https://doi.org/10.1007/s11263-009-0275-4>.
- [9] Wanling Gao, Chunjie Luo, Lei Wang, Xingwang Xiong, Jianan Chen, Tianshu Hao, Zihan Jiang, Fanda Fan, Mengjia Du, Yunyou Huang, Fan Zhang, Xu Wen, Chen Zheng, Xiwen He, Jiahui Dai, Hainan Ye, Zheng Cao, Zhen Jia, Kent Zhan, Haoning Tang, Daoyi Zheng, Biwei Xie, Wei Li, Xiaoyu Wang, and Jianfeng Zhan. AIBench: Towards Scalable and Comprehensive Datacenter AI Benchmarking. In Chen Zheng and Jianfeng Zhan, editors, *Benchmarking, Measuring, and Optimizing*, Lecture Notes in Computer Science, pages 3–9, Cham, 2019. Springer International Publishing. ISBN 978-3-030-32813-9. doi: 10.1007/978-3-030-32813-9_1.
- [10] Wanling Gao, Fei Tang, Lei Wang, Jianfeng Zhan, Chunxin Lan, Chunjie Luo, Yunyou Huang, Chen Zheng, Jiahui Dai, Zheng Cao, Daoyi Zheng, Haoning Tang, Kunlin Zhan, Biao Wang, Defei Kong, Tong Wu, Minghe Yu, Chongkang Tan, Huan Li, Xinhui Tian, Yatao Li, Junchao Shao, Zhenyu Wang, Xiaoyu Wang, and Hainan Ye. AIBench: An Industry Standard Internet Service AI Benchmark Suite, October 2019. URL <http://arxiv.org/abs/1908.08998>.
- [11] Wanling Gao, Lei Wang, Mingyu Chen, Jin Xiong, Chunjie Luo, Wenli Zhang, Yunyou Huang, Weiping Li, Guoxin Kang, Chen Zheng, Biwei Xie, Shaopeng Dai, Qian He, Hainan Ye, Yungang Bao, and Jianfeng Zhan. High fusion computers: The IoTs, edges, data centers, and humans-in-the-loop as a computer. *BenchCouncil Transactions on Benchmarks, Standards and Evaluations*, 2(3):100075, July 2022. ISSN 2772-4859. doi: 10.1016/j.tbench.2022.100075. URL <https://www.sciencedirect.com/science/article/pii/S277248592200062X>.
- [12] Amir Gholami, Sehoon Kim, Zhen Dong, Zhewei Yao, Michael W. Mahoney, and Kurt Keutzer. A Survey of Quantization Methods for Efficient Neural Network Inference, June 2021. URL <http://arxiv.org/abs/2103.13630>.

- [13] Yunchao Gong, Liu Liu, Ming Yang, and Lubomir Bourdev. Compressing Deep Convolutional Networks using Vector Quantization, December 2014. URL <http://arxiv.org/abs/1412.6115>.
- [14] Ian Goodfellow, Jean Pouget-Abadie, Mehdi Mirza, Bing Xu, David Warde-Farley, Sherjil Ozair, Aaron Courville, and Yoshua Bengio. Generative Adversarial Nets. In *Advances in Neural Information Processing Systems*, volume 27. Curran Associates, Inc., 2014. URL https://papers.nips.cc/paper_files/paper/2014/hash/5ca3e9b122f61f8f06494c97b1afccf3-Abstract.html.
- [15] Qianyu Guo, Sen Chen, Xiaofei Xie, Lei Ma, Qiang Hu, Hongtao Liu, Yang Liu, Jianjun Zhao, and Xiaohong Li. An Empirical Study Towards Characterizing Deep Learning Development and Deployment Across Different Frameworks and Platforms. In *2019 34th IEEE/ACM International Conference on Automated Software Engineering (ASE)*, pages 810–822, November 2019. doi: 10.1109/ASE.2019.00080.
- [16] Kaiming He, Xiangyu Zhang, Shaoqing Ren, and Jian Sun. Deep Residual Learning for Image Recognition. In *2016 IEEE Conference on Computer Vision and Pattern Recognition (CVPR)*, pages 770–778, June 2016. doi: 10.1109/CVPR.2016.90.
- [17] Dan Hendrycks, Collin Burns, Steven Basart, Andy Zou, Mantas Mazeika, Dawn Song, and Jacob Steinhardt. Measuring Massive Multitask Language Understanding. In *International Conference on Learning Representations*, October 2020. URL <https://openreview.net/forum?id=d7KBjmI3GmQ>.
- [18] Benoit Jacob, Skirmantas Kligys, Bo Chen, Menglong Zhu, Matthew Tang, Andrew Howard, Hartwig Adam, and Dmitry Kalenichenko. Quantization and Training of Neural Networks for Efficient Integer-Arithmetic-Only Inference. In *2018 IEEE/CVF Conference on Computer Vision and Pattern Recognition*, pages 2704–2713, June 2018. doi: 10.1109/CVPR.2018.00286.
- [19] Guofa Li, Yifan Yang, and Xingda Qu. Deep Learning Approaches on Pedestrian Detection in Hazy Weather. *IEEE Transactions on Industrial Electronics*, 67(10): 8889–8899, October 2020. ISSN 1557-9948. doi: 10.1109/TIE.2019.2945295.
- [20] Tsung-Yi Lin, Michael Maire, Serge Belongie, James Hays, Pietro Perona, Deva Ramanan, Piotr Dollár, and C. Lawrence Zitnick. Microsoft COCO: Common Objects in Context. In David Fleet, Tomas Pajdla, Bernt Schiele, and Tinne Tuytelaars, editors, *Computer Vision – ECCV 2014*, Lecture Notes in Computer Science, pages 740–755, Cham, 2014. Springer International Publishing. ISBN 978-3-319-10602-1. doi: 10.1007/978-3-319-10602-1_48.
- [21] Wei Liu, Dragomir Anguelov, Dumitru Erhan, Christian Szegedy, Scott Reed, Cheng-Yang Fu, and Alexander C. Berg. SSD: Single Shot MultiBox Detector. In Bastian Leibe, Jiri Matas, Nicu Sebe, and Max Welling, editors, *Computer Vision – ECCV 2016*, Lecture Notes in Computer Science, pages 21–37, Cham, 2016. Springer International Publishing. ISBN 978-3-319-46448-0. doi: 10.1007/978-3-319-46448-0_2.
- [22] Scott Mayer McKinney, Marcin Sieniek, Varun Godbole, Jonathan Godwin, Natasha Antropova, Hutan Ashrafian, Trevor Back, Mary Chesus, Greg S. Corrado, Ara Darzi, Mozziyar Etemadi, Florencia Garcia-Vicente, Fiona J. Gilbert, Mark Halling-Brown, Demis Hassabis, Sunny Jansen, Alan Karthikesalingam, Christopher J. Kelly, Dominic King, Joseph R. Ledlam, David Melnick, Hormuz Mostofi, Lily Peng, Joshua Jay Reicher, Bernardino Romera-Paredes, Richard Sidebottom, Mustafa Suleyman, Daniel Tse, Kenneth C. Young, Jeffrey De Fauw, and Shravya Shetty. Addendum: International evaluation of an AI system for breast cancer screening. *Nature*, 586(7829):E19–E19, October 2020. ISSN 1476-4687. doi: 10.1038/s41586-020-2679-9. URL <https://www.nature.com/articles/s41586-020-2679-9>.
- [23] Adam Paszke, Sam Gross, Francisco Massa, Adam Lerer, James Bradbury, Gregory Chanan, Trevor Killeen, Zeming Lin, Natalia Gimelshein, Luca Antiga, Alban Desmaison, Andreas Köpf, Edward Yang, Zach DeVito, Martin Raison, Alykhan Tejani, Sasank Chilamkurthy, Benoit Steiner, Lu Fang, Junjie Bai, and Soumith Chintala. PyTorch: An Imperative Style, High-Performance Deep Learning Library, December 2019. URL <http://arxiv.org/abs/1912.01703>.
- [24] Pranav Rajpurkar, Jeremy Irvin, Robyn L. Ball, Kaylie Zhu, Brandon Yang, Hershel Mehta, Tony Duan, Daisy Ding, Aarti Bagul, Curtis P. Langlotz, Bhavik N. Patel, Kristen W. Yeom, Katie Shpanskaya, Francis G. Blankenberg, Jayne Seekins, Timothy J. Amrhein, David A. Mong, Safwan S. Halabi, Evan J. Zucker, Andrew Y. Ng, and Matthew P. Lungren. Deep learning for chest radiograph diagnosis: A retrospective comparison of the CheXNeXt algorithm to practicing radiologists. *PLOS Medicine*, 15(11):e1002686, November 2018. ISSN 1549-1676. doi: 10.1371/journal.pmed.1002686. URL <https://journals.plos.org/plosmedicine/article?id=10.1371/journal.pmed.1002686>.

- [25] Vijay Janapa Reddi, Christine Cheng, David Kanter, Peter Mattson, Guenther Schmuelling, Carole-Jean Wu, Brian Anderson, Maximilien Breughe, Mark Charlebois, William Chou, Ramesh Chukka, Cody Coleman, Sam Davis, Pan Deng, Greg Diamos, Jared Duke, Dave Fick, J. Scott Gardner, Itay Hubara, Sachin Idgunji, Thomas B. Jablin, Jeff Jiao, Tom St. John, Pankaj Kanwar, David Lee, Jeffery Liao, Anton Lokhmotov, Francisco Massa, Peng Meng, Paulius Micikevicius, Colin Osborne, Genady Pekhimenko, Arun Tejusve Raghunath Rajan, Dilip Sequeira, Ashish Sirasao, Fei Sun, Hanlin Tang, Michael Thomson, Frank Wei, Ephrem Wu, Lingjie Xu, Koichi Yamada, Bing Yu, George Yuan, Aaron Zhong, Peizhao Zhang, and Yuchen Zhou. MLPerf Inference Benchmark. In *2020 ACM/IEEE 47th Annual International Symposium on Computer Architecture (ISCA)*, pages 446–459, May 2020. doi: 10.1109/ISCA45697.2020.00045.
- [26] Olga Russakovsky, Jia Deng, Hao Su, Jonathan Krause, Sanjeev Satheesh, Sean Ma, Zhiheng Huang, Andrej Karpathy, Aditya Khosla, Michael Bernstein, Alexander C. Berg, and Li Fei-Fei. ImageNet Large Scale Visual Recognition Challenge. *International Journal of Computer Vision*, 115(3):211–252, December 2015. ISSN 1573-1405. doi: 10.1007/s11263-015-0816-y. URL <https://doi.org/10.1007/s11263-015-0816-y>.
- [27] Ian Sommerville. *Software Engineering, 9/E*. Pearson Education India, 2011.
- [28] Mingxing Tan, Ruoming Pang, and Quoc V. Le. EfficientDet: Scalable and Efficient Object Detection. In *2020 IEEE/CVF Conference on Computer Vision and Pattern Recognition (CVPR)*, pages 10778–10787, June 2020. doi: 10.1109/CVPR42600.2020.01079.
- [29] Tolga Turay and Tanya Vladimirova. Toward Performing Image Classification and Object Detection With Convolutional Neural Networks in Autonomous Driving Systems: A Survey. *IEEE Access*, 10:14076–14119, 2022. ISSN 2169-3536. doi: 10.1109/ACCESS.2022.3147495.
- [30] Ashish Vaswani, Noam Shazeer, Niki Parmar, Jakob Uszkoreit, Llion Jones, Aidan N Gomez, Łukasz Kaiser, and Illia Polosukhin. Attention is All you Need. In *Advances in Neural Information Processing Systems*, volume 30. Curran Associates, Inc., 2017. URL https://papers.nips.cc/paper_files/paper/2017/hash/3f5ee243547dee91fbd053c1c4a845aa-Abstract.html.
- [31] Jindong Wang, Cuiling Lan, Chang Liu, Yidong Ouyang, and Tao Qin. Generalizing to Unseen Domains: A Survey on Domain Generalization. In *Twenty-Ninth International Joint Conference on Artificial Intelligence*, volume 5, pages 4627–4635, August 2021. doi: 10.24963/ijcai.2021/628. URL <https://www.ijcai.org/proceedings/2021/628>.
- [32] Benjamin Wolfe, Bobbie Seppelt, Bruce Mehler, Bryan Reimer, and Ruth Rosenholtz. Rapid holistic perception and evasion of road hazards. *Journal of Experimental Psychology. General*, 149(3):490–500, March 2020. ISSN 1939-2222. doi: 10.1037/xge0000665.
- [33] Benjamin Wolfe, Anna Kosovicheva, Simon Stent, and Ruth Rosenholtz. Effects of temporal and spatiotemporal cues on detection of dynamic road hazards. *Cognitive Research: Principles and Implications*, 6(1):80, December 2021. ISSN 2365-7464. doi: 10.1186/s41235-021-00348-4. URL <https://doi.org/10.1186/s41235-021-00348-4>.
- [34] Huazhe Xu, Yang Gao, Fisher Yu, and Trevor Darrell. End-to-End Learning of Driving Models from Large-Scale Video Datasets. In *2017 IEEE Conference on Computer Vision and Pattern Recognition (CVPR)*, pages 3530–3538, July 2017. doi: 10.1109/CVPR.2017.376.
- [35] Ekim Yurtsever, Jacob Lambert, Alexander Carballo, and Kazuya Takeda. A Survey of Autonomous Driving: Common Practices and Emerging Technologies. *IEEE Access*, 8:58443–58469, 2020. ISSN 2169-3536. doi: 10.1109/ACCESS.2020.2983149.
- [36] Jianfeng Zhan. A BenchCouncil view on benchmarking emerging and future computing. *Bench-Council Transactions on Benchmarks, Standards and Evaluations*, 2(2):100064, April 2022. ISSN 2772-4859. doi: 10.1016/j.tbench.2022.100064. URL <https://www.sciencedirect.com/science/article/pii/S2772485922000515>.
- [37] Tao Zhang and Zhenhua Tan. Deep Emotion Recognition using Facial, Speech and Textual Cues: A Survey, October 2021. URL https://www.techrxiv.org/articles/preprint/Deep_Emotion_Recognition_in_Dynamic_Data_using_Facial_Speech_and_Textual_Cues_A_Survey/15184302/2.
- [38] Lianmin Zheng, Wei-Lin Chiang, Ying Sheng, Siyuan Zhuang, Zhonghao Wu, Yonghao Zhuang, Zi Lin, Zhuohan Li, Dacheng Li, Eric P. Xing, Hao Zhang, Joseph E. Gonzalez, and Ion Stoica. Judging LLM-as-a-judge with MT-Bench and Chatbot Arena, July 2023. URL <http://arxiv.org/abs/2306.05685>.
- [39] Kaiyang Zhou, Ziwei Liu, Yu Qiao, Tao Xiang, and Chen Change Loy. Domain Generalization: A Survey. *IEEE Transactions on Pattern Analysis and Machine Intelligence*, 45(4):4396–4415, April 2023. ISSN 1939-3539. doi: 10.1109/TPAMI.2022.3195549.